Am J Physiol Lung Cell Mol Physiol 308: L358–L367, 2015.
First published December 12, 2014; doi:10.1152/ajplung.00341.2014.

CALL FOR PAPERS | *Biomarkers in Lung Diseases: from Pathogenesis to Prediction to New Therapies*

Distinct macrophage phenotypes in allergic and nonallergic lung inflammation

Patricia Robbe,[1,2] Christina Draijer,[2,3] Thiago R. Borg,[1,2] Marjan Luinge,[1,2] Wim Timens,[1,2] Inge M. Wouters,[4] Barbro N. Melgert,[2,3] and Machteld N. Hylkema[1,2]

[1]*University of Groningen, University Medical Center Groningen, Department of Pathology, Groningen, The Netherlands;* [2]*University of Groningen, University Medical Center Groningen, GRIAC- Groningen Research Institute for Asthma and COPD, Groningen, The Netherlands;* [3]*University of Groningen, Department of Pharmacokinetics, Toxicology and Targeting, Groningen, The Netherlands;* [4]*Institute for Risk Assessment Sciences (IRAS), Division of Environmental Epidemiology, University of Utrecht, Utrecht, The Netherlands*

Submitted 13 November 2014; accepted in final form 11 December 2014

Robbe P, Draijer C, Borg TR, Luinge M, Timens W, Wouters IM, Melgert BN, Hylkema MN. Distinct macrophage phenotypes in allergic and nonallergic lung inflammation. *Am J Physiol Lung Cell Mol Physiol* 308: L358–L367, 2015. First published December 12, 2014; doi:10.1152/ajplung.00341.2014.—Chronic exposure to farm environments is a risk factor for nonallergic lung disease. In contrast to allergic asthma, in which type 2 helper T cell (Th2) activation is dominant, exposure to farm dust extracts (FDE) induces Th1/Th17 lung inflammation, associated with neutrophil infiltration. Macrophage influx is a common feature of both types of lung inflammation, allergic and nonallergic. However, macrophage functions and phenotypes may vary according to their polarized state, which is dependent on the cytokine environment. In this study, we aimed to characterize and quantify the lung macrophage populations in two established murine models of allergic and nonallergic lung inflammation by means of fluorescence-activated cell sorting and immunohistochemistry. We demonstrated that, whereas in allergic asthma M2-dominant macrophages predominated in the lungs, in nonallergic inflammation M1-dominant macrophages were more prevalent. This was confirmed in vitro using a macrophage cell line, where FDE exerted a direct effect on macrophages, inducing M1-dominant polarization. The polarization of macrophages diverged depending on the exposure and inflammatory status of the tissue. Interfering with this polarization could be a target for treatment of different types of lung inflammation.

macrophages; allergic asthma; farm dust; nonallergic asthma

EXPOSURE TO FARM ENVIRONMENTS can induce respiratory diseases, such as nonallergic asthma, chronic bronchitis, and chronic obstructive respiratory disease (5). We and others have shown that exposure to farm dust extract (FDE) induces a marked nonallergic type of lung inflammation with infiltration of neutrophils, macrophages, and T helper type 1 (Th1) and Th17 cells into mice lungs (22, 25). Allergic asthma is typically a Th2-type disease characterized by the presence of Th2 cells, eosinophils, macrophages, and cytokines, such as interleukin (IL)-4, IL-5, and IL-13 (30). Interestingly, a common feature of both allergic and nonallergic asthma is the increased numbers of macrophages in the lungs.

Lung macrophages are important innate immune cells, which play critical roles in lung homeostasis, host defense against pathogens, and resolution of inflammation. These diverse functions of macrophages are achieved by the plasticity of these cells, which, depending on signals present in their microenvironment, can polarize into a plethora of different phenotypes (14, 28). Cytokines, such as interferon (IFN)-γ and tumor necrosis factor (TNF)-α, or bacterial products, such as lipopolysaccharide (LPS), induce polarization into proinflammatory macrophages through the transcription factor IFN-regulatory factor 5 (IRF5). These macrophages, loosely called M1-dominant macrophages, release proinflammatory cytokines IL-12, IL-1β, and TNF-α and are important in host defense against intracellular pathogens (9, 14).

Macrophages induced by the proallergic asthma cytokines IL-4 and IL-13, also known as M2-dominant macrophages, are important in wound healing and host defense against helminth infections and are characterized by upregulation of the mannose receptor (CD206) and, in mice, production of the chitinase-like protein YM1. Anti-inflammatory macrophages are induced by compounds and mediators like corticosteroids, IL-10, or PGE2. These anti-inflammatory macrophages are also characterized by upregulation of CD206 but produce the anti-inflammatory cytokine IL-10 (1).

We and others have shown that asthmatics (12) and mice with allergic airway inflammation have higher numbers of M2-dominant macrophages and their products in lung tissue (7, 11, 12, 15), serum, and bronchoalveolar lavage (BAL) (3) compared with controls. In addition, numbers of this macrophage phenotype have been associated with disease severity both in mice and humans (4, 12), and these macrophages may contribute to the development of allergic airway inflammation (6, 10, 11, 13).

In mice exposed to FDE, we and others noticed higher numbers of macrophages in lung tissue (19, 25). However, the phenotype of these macrophages has not been investigated yet. In this study, we therefore compared macrophage phenotypes in allergic and nonallergic lung inflammation and used a macrophage cell line to investigate the direct effect of FDE exposure on macrophage polarization.

Address for reprint requests and other correspondence: P. Robbe, Hanzeplein 1, 9713 GZ Groningen, Dept. of Pathology EA10, 050-3611285 (e-mail: p.robbe@umcg.nl).

MATERIALS AND METHODS

FDE. Settled dust samples ($n = 30$) were collected from ridges in multiple cattle farms. Dust was pooled, and FDE was prepared as described previously (25). Briefly, aliquots of ~2.5 g of pooled dust were mixed with 12.5-g glass beads, and sterile water was added to a volume of 50 ml in a Greiner tube, mixed for 5 min on an end-over-end roller at room temperature, and subsequently sonicated for 5 min in an ultrasonic bath with crushed ice. Afterward, aliquots were pooled in a glass Erlenmeyer flask, and sterile water was added to a final concentration of 10 mg dust per ml; sodium chloride solution was added until a final concentration of 0.9% was reached. Erlenmeyers were shaken for 6 h at room temperature. Samples were then centrifuged at 20,000 *g* at 4°C for 45 min, and after centrifugation the dust extract was dialyzed (MWCO 3500) against deionized distilled water, sterilized through filtration through a 0.22-μm filter, and lyophilized.

Endotoxin concentration of FDE was assessed using the limulus amebocyte lysate assay (Lonza, Verviers, Belgium) as described previously (25). One milligram per milliliter of FDE contained 9,941 endotoxin units (EU) per milligram.

Animals. Specific pathogen-free female BALB/c mice (aged 6–8 wk; Harlan, Horst, The Netherlands) were housed in groups of 6–8 mice each and had access to standard food and water ad libitum. An established model for intranasal instillation of FDE or house dust mite (HDM, whole bodies from *Dermatophagoides pteronyssinus*; Greer Laboratories, Lenoir, NC) was used (25). Briefly, mice were anesthetized with isofluorane and intranasally exposed to FDE (1 mg/ml in PBS, 50 μl/day), HDM (40 μg/day in 50 μl PBS), or sterile PBS (50 μl/day) as a control, four times per week, during six consecutive weeks. All animal protocols were approved by the Institutional Animal Care and Use Committee of the University of Groningen (Permit Number: 6615A), and procedures were performed under strict governmental and international guidelines.

Tissue collection. After 6 wk of exposure to either HDM or FDE, mice were anaesthetized and killed by cardiac exsanguination. From eight mice per group, the left lung lobe was snap frozen and kept in −80°C until preparation of lung homogenates for cytokine analysis. Right lung lobes were carefully inflated with 0.9 ml 50% Tissue Tek, optimal cutting temperature compound (SaKura, Alphen aan den Rijn, The Netherlands) in PBS, and three of the four lobes were snap frozen and stored at −80°C until use, while the smallest right lung lobe was formalin fixed and embedded in paraffin. From six mice per group, lungs were removed and kept in cold PBS for lung cell isolation.

Lung homogenates. Snap-frozen lung tissue was mechanically homogenized (50% wt/vol) in 50 mM Tris·HCl buffer, containing 150 mM NaCl, 0.002% Tween-20 (pH 7.5), and a protease inhibitor (Sigma Aldrich, Zwijndrecht, The Netherlands). Homogenates were centrifuged at 12,000 *g* for 10 min to remove any insoluble material. Supernatants were subsequently stored at −80°C until further analysis.

Lung cell isolation. Lungs were minced and incubated for 45 min at 37°C in RPMI medium supplemented with 10% fetal calf serum (both Lonza, Verviers, Belgium), 10 μg/ml DNAse I (grade II from bovine pancreas; Roche Applied Science, Almere, The Netherlands), and 0.7 mg/ml collagenase A (Sigma Aldrich) in a shaking water bath. After that, the digested lung tissue was passed through a 70-μm nylon strainer (BD Biosciences, Breda, The Netherlands) to obtain single-cell suspensions. To lyse contaminating erythrocytes, cell suspensions were incubated with 10 times diluted Pharmlyse (BD Biosciences). Cells were centrifuged through 70-μm strainer caps and counted using a pocH-100i hematology analyzer (Sysmex, Mundelein, IL) before they were used for flow cytometry.

Flow cytometric analysis. Single lung cell suspensions were stained for macrophage subsets using the following directly labeled antibodies: allophycocyanin (APC)/Cy7-conjugated anti-CD11c (Biolegend, Fell, Germany), Percp/Cy5.5-conjugated anti-CD11b (Biolegend), PE-conjugated anti-CD206 (Biolegend), A700-conjugated anti-major histocompatibility complex (MHC) class II (Biolegend), Pacific Blue-conjugated anti-F4/80 (Biolegend), and Alexa Fluor 647-conjugated anti-ICAMI (Biolegend).

Approximately 10^6 cells were incubated with the antibody mix including 1% normal mouse serum for 30 min on ice, protected from light. After washing the cells with PBS supplemented with 2% FCS and 5 mM EDTA (PFE), we incubated the cells with fluorescence-activated cell sorting (FACS) lysing solution (BD Biosciences) for 30 min on ice. After that, cells were washed once with PFE and resuspended in PFE and kept in the dark on ice until flow cytometric analysis. The fluorescent staining of the cells was measured on a LSR-II flow cytometer (BD Biosciences), and data were analyzed using FlowJo Software (Tree Star, Ashland, OR).

Cytokine analysis. Concentrations of cytokines were measured in lung homogenates by multiplex ELISA system (Affimetrix, High Wycombe, UK). Cytokines measured were as follows: IL-1β [lower limit of detection (LLD) = 0.16 pg/ml], IL-4 (LLD = 0.11 pg/ml), IL-5 (LLD = 0.22 pg/ml), IL-10 (LLD = 0.75 pg/ml), IL-12p70 (LLD = 0.13 pg/ml), IL-13 (LLD = 0.23 pg/ml), IL-17A (LLD = 0.08 pg/ml), TNF-α (LLD = 0.12 pg/ml), and IFN-γ (LLD = 0.1 pg/ml). YM1 (LLD = 60.1 pg/ml) was measured in lung homogenate by standard ELISA (R&D Systems, Oxon, UK).

Histology. Sections (3 μm) of formalin-fixed and paraffin-embedded lung tissue were stained for different macrophage subsets using a general macrophage marker, Mac3 (rat anti-Mac3, BD Biosciences), in combination with phenotype-specific markers using standard immunohistochemical procedures. To visualize Mac3, an immunoalkaline phosphatase procedure was used with Fast Blue BB salt (Sigma Aldrich) as chromogen. Numbers of M1-dominant macrophages were determined by double staining of Mac3 and IRF5 (rabbit anti-IRF5; Proteintech Europe, Manchester, UK); M2-dominant macrophages were determined by double staining of Mac3 and YM1 [goat anti-mouse eosinophil chemotactic factor (ECF-L), R&D Systems]; anti-inflammatory macrophages were identified by double staining of Mac3 and IL-10 (rabbit anti-IL-10; Hylcult Biotech, Uden, The Netherlands). IRF5, YM1, and IL-10 were visualized with 3-amino-9-ethylcarbazole (Sigma Aldrich) as chromogen. Double-positive cells were counted manually in parenchymal lung tissue, and numbers were corrected for the total area of lung tissue section as assessed by morphometric analysis using Aperio ImageScope viewing software 11.2.0.780 (Aperio, Vista, CA).

RAW cells culture. RAW 264.7 macrophages (EACC, Salisbury, UK) were cultured in DMEM (Invitrogen, Gaithersburg, MD) enriched with 10% fetal calf serum, 10 μg/ml Gentamycin (Invitrogen) and 2 mM L-glutamine (Invitrogen). Cultures were split 1:4–1:8 twice a week, with careful scraping in their old medium. They were then transferred to a new T75 culturing flask (Corning, Corning, NY), with new medium.

RAW 264.7 macrophages in *passage 9–12* were cultured in 12-well plates using DMEM (Invitrogen) enriched with 10% fetal calf serum, 10 μg/ml gentamycin (Invitrogen), and 2 mM L-glutamine (Invitrogen). Macrophages were stimulated, using either IFN-γ (10 ng/ml; PeproTech, Rocky Hill, NJ), IL-13 (10 ng/ml, PeproTech), PGE2 (5 μM, PeproTech), or FDE at the concentrations of 1 μg/ml, 50 μg/ml, and 100 μg/ml for 48 h.

After stimulation, cells were collected for the flow cytometry analysis. Cells were incubated with 4 mg/ml Lidocaine, 10 mM EDTA, and 10% fetal calf serum in phosphate-buffered saline solution (pH 7.3) for 15 min. They were detached by vigorous pipetting and transferred into 1.5 ml tubes. Cells were washed three times with PFE before they were used for flow cytometry.

Flow cytometric analysis of RAW cells. Membrane staining was performed using APC/Cγ7-conjugated anti-MHC class II antibody (Biolegend) and Alexa Fluor 647-conjugated anti-CD206 antibody (Biolegend) with a 30-min incubation in the dark, on ice. After being washed three times using cold PFE, cells were fixed and permeabil-

ized for 30 min in cold Fix/Perm buffer (BD Biosciences) and then washed with cold permeabilization buffer (BD Biosciences). After that, cells were incubated for 30 min in the dark with PE-conjugated anti-IL-10 antibody (eBioscience, Vienna, Austria) for intracellular staining. After the incubation, cells were washed twice in permeabilization buffer and then were resuspended in PFE. An appropriate isotype control was used for the IL-10 staining (rat IgG2bκ-PE, eBiosciences).

Analysis was performed using a BD FACSArray cytometer (BD Biosciences), and data were analyzed using FlowJo software (Tree Star). Mean fluorescence intensity was used to evaluate the expression of the different markers.

Microscopy of RAW cells. Cell cultures were photographed before each flow cytometric analysis to observe changes in morphology that could be related to changes in the milieu.

Pictures of the cells were made using an Olympus IX50 microscope (Olympus, Tokyo, Japan). Images were manually focused around the middle point between the center of the well and the border of it. The brightness, contrast, and the color saturation settings were automatically calibrated by the capture program Cell^{A} (Olympus), which was also used to obtain the images.

Statistical methods. Nonparametric Kruskal-Wallis test was used to assess whether differences between groups existed, and, when $P < 0.05$, Mann-Whitney *U*-test was performed to assess differences between subgroups. All analyses were performed using GraphPad Prism 5.0, and differences were considered statistically significant at two-sided *P* values <0.05. $P < 0.10$ was considered a statistical trend.

RESULTS

HDM and FDE induce differential types of activated CD11c+/ CD11b+ alveolar macrophages in the lungs. To identify macrophage phenotypes, six-color FACS analysis was performed. Macrophages were first identified based on autofluorescence and F4/80 expression. Total numbers of macrophages were higher in mice exposed to HDM compared with PBS-exposed mice, and this number was even higher in FDE-exposed mice (Fig. 1*A*). Alveolar macrophage numbers, identified by high autofluorescence and CD11c expression, were also higher in HDM-exposed mice compared with PBS-exposed mice and increased even further in FDE-exposed mice (Fig. 1*B*). Alveolar macrophages are known to lack expression of the adhesion molecule CD11b, except when they are activated or represent recruited macrophages (8). Activated alveolar macrophages, defined as $CD11c^{+}CD11b^{+}$, were previously shown to be increased after repetitive organic dust exposure (19). Within the $CD11c^{+}$-positive population, we found that numbers of cells expressing CD11b were higher in HDM-exposed mice than in control mice and even higher in FDE-exposed mice.

To determine the type of tissue signals that these activated alveolar macrophages have seen in each type of inflammation, we analyzed the expression of intracellular adhesion molecule 1 (ICAM-1), a marker of M1-dominant macrophages (8), and CD206 (mannose receptor), a marker of M2-dominant macrophages (26). HDM exposure induced higher expression of CD206 in $CD11c^{+}CD11b^{+}$ cells, whereas both HDM and FDE induced ICAM-1 expression in these cells, compared with control mice. Of note, FDE exposure induced higher expression of ICAM-1 than HDM exposure but did not induce CD206 expression (Fig. 1, *D* and *E*). These results demonstrate that, although numbers of total macrophages, alveolar macrophages, and activated alveolar macrophages are increased in different types of lung inflammation, the phenotype, and thus the function of the macrophages, may be different depending on the type of inflammation.

Predominant macrophage phenotypes vary according to the type of inflammation. To further study the presence of the different macrophage phenotypes in lung tissue after HDM and FDE exposure, lung sections were stained for macrophages with a general macrophage marker (Mac3) in combination with more specific markers for macrophage subsets. M1-dominant macrophages were identified as $IRF5^{+}Mac3^{+}$ cells; M2-dominant macrophages were identified as $YM1^{+}Mac3^{+}$ cells; anti-inflammatory macrophages were characterized as $IL\text{-}10^{+}Mac3^{+}$ cells. Interestingly, although HDM-exposed mice had more M1-dominant macrophages in the lungs than PBS-exposed mice, FDE-exposed mice had the highest numbers of M1-dominant macrophages of all groups (Fig. 2*A*). In contrast, M2-dominant macrophage numbers were the highest in lungs of mice exposed to HDM, whereas FDE-exposed mice still had more M2-dominant macrophages than PBS control mice (Fig. 2*B*). Anti-inflammatory macrophage numbers were significantly lower in lungs from both HDM- and FDE-exposed mice, compared with PBS-exposed mice (Fig. 2*C*).

Furthermore, cytokines were measured in lung homogenates, and we found that levels of the M1-related cytokines TNF-α and IL-1β were higher in lung tissue of FDE-exposed mice than in PBS- and HDM-exposed mice (Fig. 3, *A* and *B*). YM1 levels were increased in HDM-exposed mice compared with PBS- and FDE-exposed mice (Fig. 3*C*). IL-10 levels were increased in both HDM- and FDE-exposed mice compared with control mice (Fig. 3*D*), suggesting that the main source of IL-10 in these mice lungs is not macrophages.

To confirm that the HDM and FDE models have induced Th2 and Th17 lung inflammation, Th2 cytokines and IL-17 were also measured in lung tissue. Levels of IL-4, IL-5, and IL-13 were significantly higher in HDM-exposed mice compared with PBS- and FDE-exposed mice. IL-17A levels were the highest in FDE-exposed mice compared with both HDM-exposed mice and controls. HDM also had more IL-17A than PBS mice. Because it has been shown that FDE exposure can induce Th1 cytokines in mouse lungs (18), levels of IL-12p70 and IFN-γ were also measured. Levels of IL-12p70 were higher in HDM-exposed mice compared with PBS-exposed mice. With respect to IFN-γ, similar levels were found in the different groups (Table 1).

Macrophages polarize into M1-dominant, M2-dominant, or anti-inflammatory subsets depending on the in vitro cytokine stimulation. To evaluate the polarization of macrophages in vitro, RAW cells were incubated for 48 h with IFN-γ, IL-13, and PGE2 to induce M1-dominant, M2-dominant, and anti-inflammatory phenotypes, respectively. Polarization of macrophages into the different phenotypes was assessed by flow cytometric analysis of MHC class II (M1-dominant subset), CD206 (M2-dominant subset), and IL-10 (anti-inflammatory subset). IFN-γ stimulation induced MHC class II expression (trend $P = 0.0571$, Fig. 4*A*), whereas IL-13 and PGE2 stimulation induced CD206 expression (Fig. 4*B*) and IL-10 expression (Fig. 4*C*).

Farm dust induces M1-dominant but not M2-dominant or anti-inflammatory macrophages in vitro. RAW cells were stimulated with FDE in concentrations of 1 μg/ml, 50 μg/ml, and 100 μg/ml to investigate the direct effect of FDE exposure on macrophage polarization. FDE stimulation dose depend-

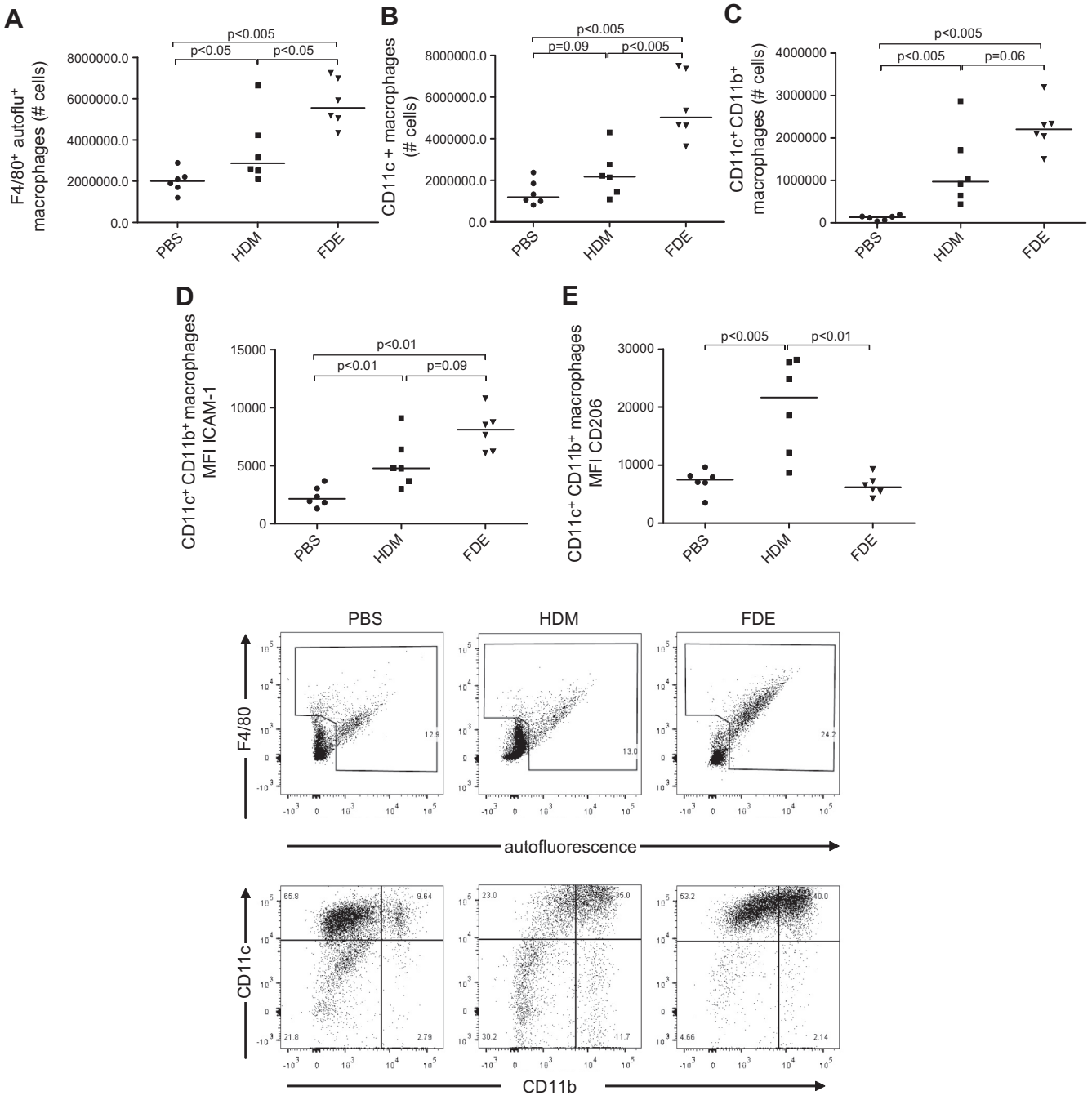

Fig. 1. House dust mite (HDM) and farm dust extract (FDE) induce different phenotypes of activated CD11c+/CD11b+ macrophages in the lungs. Mice were exposed to PBS, HDM, or FDE 4 times/week for 6 consecutive wk, and lung cells were isolated and stained for fluorescence-activated cell sorting analysis. Scatter dot plots showing median and distribution of numbers of F4−80$^+$/autoflu$^+$ macrophages (*A*), numbers of CD11c$^+$ cells within macrophage population (*B*), and numbers of CD11b$^+$ cells within the CD11c$^+$ population (*C*). Mean fluorescence intensity (MFI) of surface markers ICAM-1 (*D*) and CD206 (*E*) on gated CD11c$^+$CD11b$^+$ cells are shown. Representative dot plots of lung cells of PBS-, HDM-, and FDE-exposed mice are shown.

ently induced MHC class II expression, whereas CD206 or IL-10 expressions were not induced (Fig. 5, *A*–*C*).

DISCUSSION

This study demonstrates that, in response to different types of exposures, different types of macrophages are present in the lungs and that the predominant phenotype varies according to the type of inflammation. In our FDE model of nonallergic lung inflammation, the M1-dominant phenotype predominates, whereas, in the HDM model of allergic inflammation, M2-dominant macrophages are more prevalent. Furthermore, we showed that in vitro FDE exposure of RAW macrophages directly induced M1-dominant polarization, whereas it did not induce M2-dominant or anti-inflammatory macrophages.

Two established models of lung inflammation were used to study the relative distribution of macrophage phenotypes, one model of HDM-induced allergic lung inflammation and one FDE model of nonallergic lung inflammation. Allergic inflam-

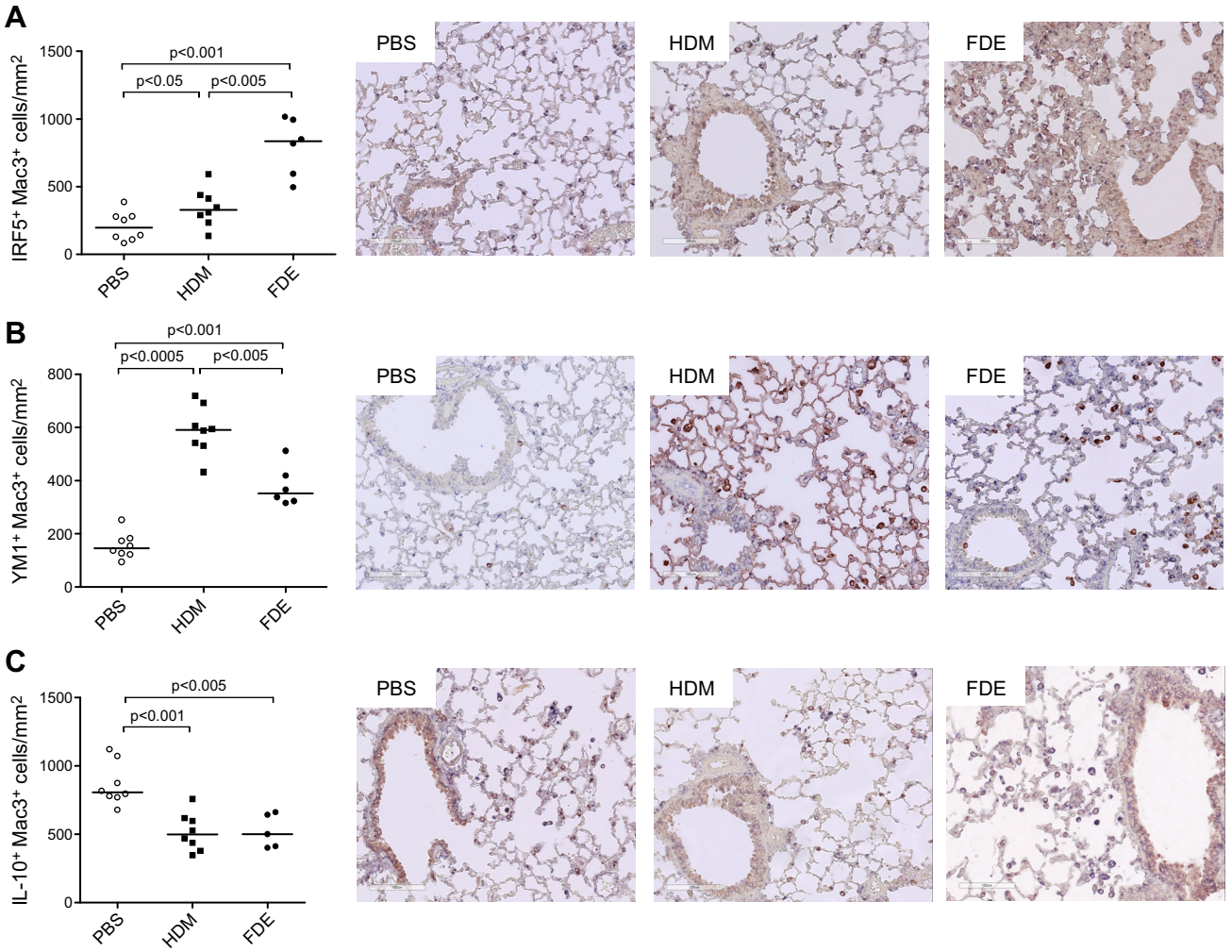

Fig. 2. Predominant macrophage phenotypes vary with the type of exposure. Scatter dot plots showing median and distribution of numbers of IFN-regulatory factor (IRF)5$^+$Mac3$^+$ cells (A), YM1$^+$Mac3$^+$ cells (B), and IL-10$^+$Mac3$^+$ cells (*C*) in lung tissue of mice exposed to PBS, HDM, or FDE 4 times/week for 6 consecutive weeks. Representative pictures of immunohistochemical stainings are shown for all 3 double stainings of PBS, HDM, and FDE groups.

mation relates typically to a Th2-type response, with high numbers of eosinophils in the lungs, high levels of serum IgE, and Th2 cytokines. In contrast, FDE exposure was shown to induce chronic infiltration of Th1/Th17/Tc17 cells and lung neutrophilia in the mouse (18, 25). A common feature of both models is the presence of increased numbers of macrophages in the lungs (4, 22). Here we show that, comparing both models, the FDE model has larger numbers of total macrophages in the lungs, larger numbers of CD11c$^+$ macrophages, and larger numbers of activated CD11c$^+$/CD11b$^+$ macrophages than is found in the HDM model. Of interest, when we focused on the phenotype of these cells, we found that macrophages differ in phenotype depending on the type of exposure and inflammation. Nonallergic inflammation was accompanied by higher numbers of macrophages with the M1-dominant phenotype, whereas the M2-dominant phenotype was relatively more present in allergic inflammation.

The distinctive macrophage populations in our study were identified using specific markers for each subset. By means of flow cytometry, ICAM-1 expression was used to identify M1-dominant macrophages (8) and CD206 expression to identify the M2-dominant subset. Because the mannose receptor (CD206) is expressed by both M2-dominant and anti-inflammatory macrophages, an additional marker is required to identify both subsets. This was accomplished by immunohistochemistry, where double stainings were performed for Mac3 (general macrophage marker) in combination with IRF5, YM1, or IL-10 to identify M1-dominant, M2-dominant, and anti-inflammatory macrophages, respectively. IRF5 has been shown to be a specific marker for M1-dominant macrophages in vivo and in vitro (9, 27), inducing transcription of genes encoding IL-12 and IL-23 and suppressing the gene encoding IL-10 in diverse disease settings. YM1 is a unique marker for M2-dominant macrophages in the lung (4, 23). To identify anti-inflammatory macrophages, also known as regulatory macrophages, we chose to investigate the expression of the immunosuppressive cytokine IL-10, which is the most important characteristic of this type of macrophages (14). Considering that IL-10 can be produced by different cell types, the use of a double staining with Mac3 was pivotal to characterize anti-inflammatory macrophages.

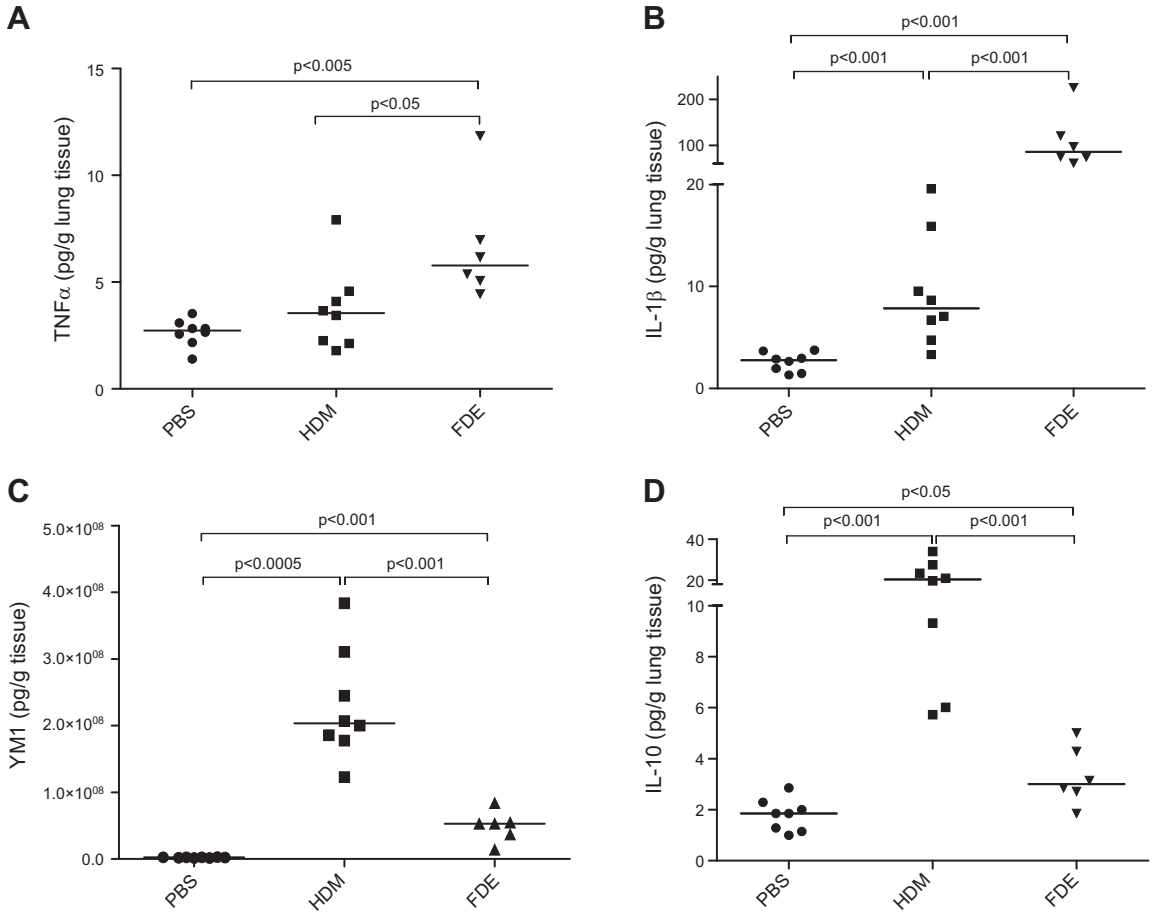

Fig. 3. Scatter dot plots showing median and distribution of levels of TNF-α (*A*), IL-1β (*B*), YM1 (*C*), and IL-10 (*D*) in lung tissue of mice exposed to PBS, HDM, or FDE 4 times/week for 6 consecutive weeks.

We found increased numbers of IRF5-expressing macrophages after FDE exposure. Because the transcription factor IRF5 has been shown to directly activate transcription of IL-12 and IL-23 in macrophages and subsequently promote T cell differentiation of Th1 and Th17 lineages (9), it is tempting to speculate that M1-dominant macrophages are involved in the initiation of the adaptive nonallergic immune response, as observed in individuals occupationally exposed to farm environments and in our mouse model of FDE exposure. On the other hand, a critical role of macrophages in downregulation of inflammatory responses has been shown by Poole and coworkers (19), after prolonged exposure to FDE from a swine facility. The authors showed that depletion of macrophages before and during FDE exposure enhanced lung neutrophil infiltration. Although the different macrophages were not phenotyped in that study, induction of M1-dominant cytokines TNF-α and IL-6 by FDE was greatly diminished after macrophage depletion, suggesting presence of, in particular, M1-dominant macrophages in the FDE model.

Table 1. *Th1, Th2, and Th17 cytokines in lung tissue*

	PBS	HDM	FDE
		Th1 cytokines	
IL-12p70	0.44 (0.13–0.67)	0.92 (0.40–1.84)*	0.46 (0.33–0.98)
IFN-γ	1.75 (0.69–4.37)	2.52 (0.77–11.30)	1.55 (0.93–4.92)
		Th2 cytokines	
IL-4	0.15 (0.12–0.28)	22.34 (7.21–51.07)‡	2.56 (1.58–5.44)†§
IL-5	0.48 (0.28–1.39)	32.30 (7.17–122.20)‡	1.47 (0.84–3.47)*§
IL-13	0.24 (0.11–5.07)	18.85 (8.66–82.69)‡	2.23 (0.71–3.37)*§
		Th17 cytokine	
IL-17	0.81 (0.35–3.45)	8.72 (1.67–23.49)‡	47.14 (12.60–119.90)‡§

Values are medians, pg/g tissue (range). Subgroup analysis: house dust mite (HDM) vs. PBS or farm dust extract (FDE) vs. PBS groups: *$P < 0.05$; †$P < 0.01$; ‡$P < 0.001$. HDM vs. FDE groups: §$P < 0.001$. Th1, T helper type 1.

In HDM-exposed mice, higher numbers of M2-dominant macrophages and higher levels of its chemokine YM1 were found compared with control or FDE-exposed mice, which is in agreement with previous studies (4, 11, 12). YM1 is also known as ECF-L, and we have previously shown that YM1 levels in BAL fluid (BALF) strongly correlated with eosinophils in BALF (4). With respect to anti-inflammatory macrophages, the highest numbers of these cells were found in control mice, reproducing our previous findings (4). Strikingly, IL-10 levels were increased in both HDM- and FDE-exposed mice compared with control mice, suggesting that the main source of IL-10 in these mice lungs is not macrophages. An obvious other candidate for this would be regulatory T cells, which are known IL-10 producers (24). We have previously

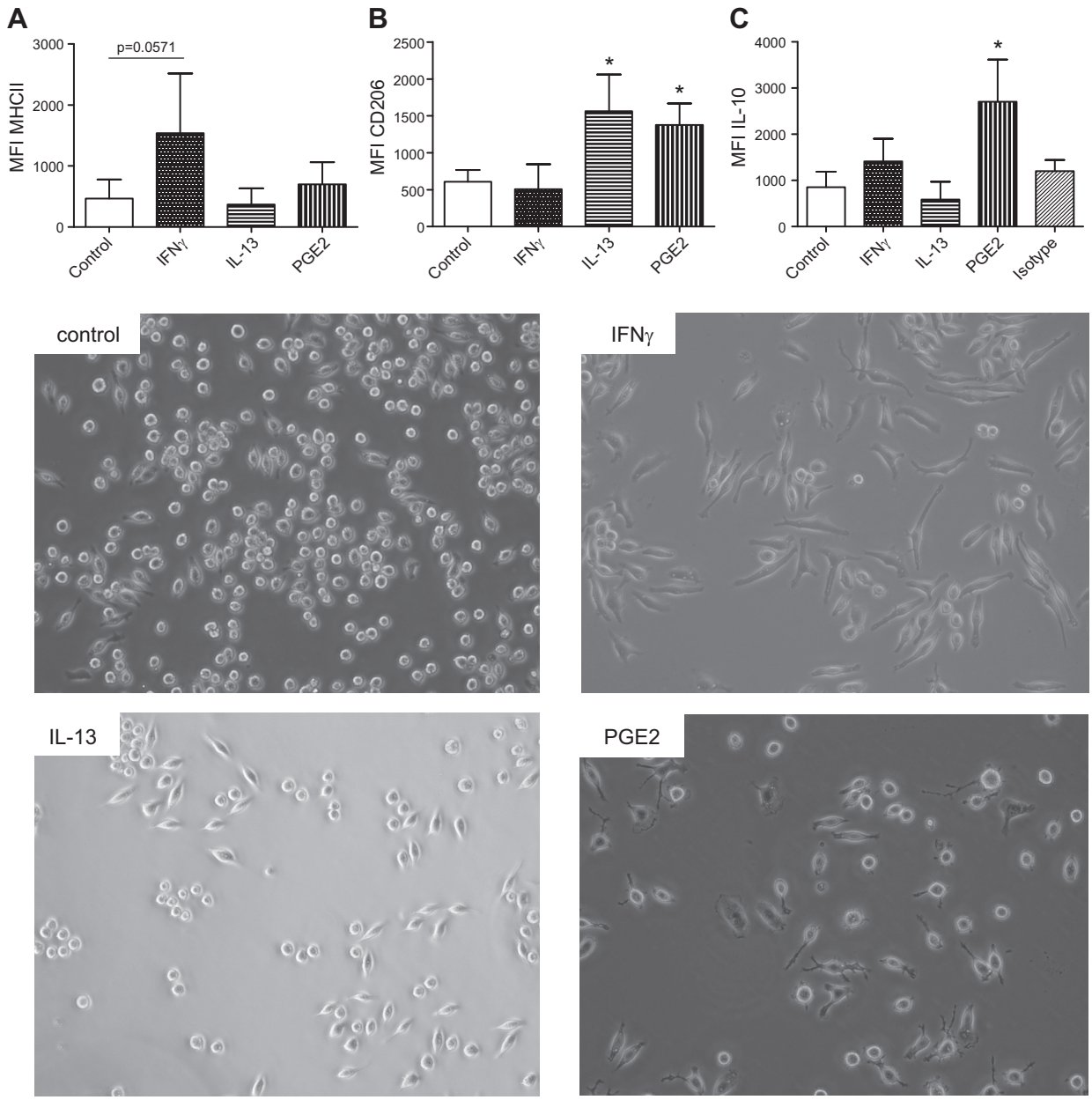

Fig. 4. Macrophages polarize into M1-dominant, M2-dominant, and anti-inflammatory macrophages in response to IFN-γ, IL-13, and PGE2 stimulations, respectively. Bar graphs of MFI of major histocompatibility complex II (MHC II) (M1-dominant subset) (*A*), CD206 (M2-dominant subset) (*B*), and IL-10 (anti-inflammatory subset) (*C*) of RAW cells stimulated with IFN-γ, IL-13, or PGE2 for 48 h. Each bar displays the mean and SD of 4 independent experiments. Representative pictures of RAW cells are shown from control group, and IFN-γ-, IL-13-, or PGE2-stimulated groups. $*P < 0.05$ compared with control.

shown increased numbers of regulatory T cells in HDM-exposed mice (4). Other candidates for IL-10 production are B cells, which should be the subject of future studies in our models.

Our findings in the mouse were confirmed in vitro, as FDE exclusively induced M1-dominant polarization, and suggest that FDE exposure in vivo exerts a direct effect on macrophages, which may be independent of other cell types or mediators. This direct effect occurs probably through activation of pattern-recognition receptors (PRRs) on macrophages by microbial components present in the FDE. LPS, a major component of the cell wall of Gram-negative bacteria, is recognized by the PRR Toll-like receptor 4 (TLR4), and it is known to be present in FDE, as well as muramic acid, a peptidoglycan derived predominantly from Gram-positive bacteria, which activates TLR2 and nucleotide oligomerization domain 2 (20, 21). Moreover, it has been shown in monocyte-derived macrophages that FDE exposure induces TNF-α production (17), which can induce M1-dominant polarization. In addition to TLR activation-induced TNF transcription, some TLR ligands can activate Toll/IL-1 receptor domain-containing-adaptor protein inducing IFN-β-dependent pathways, resulting in IFN-β production (29). This endogenously produced IFN-β can re-

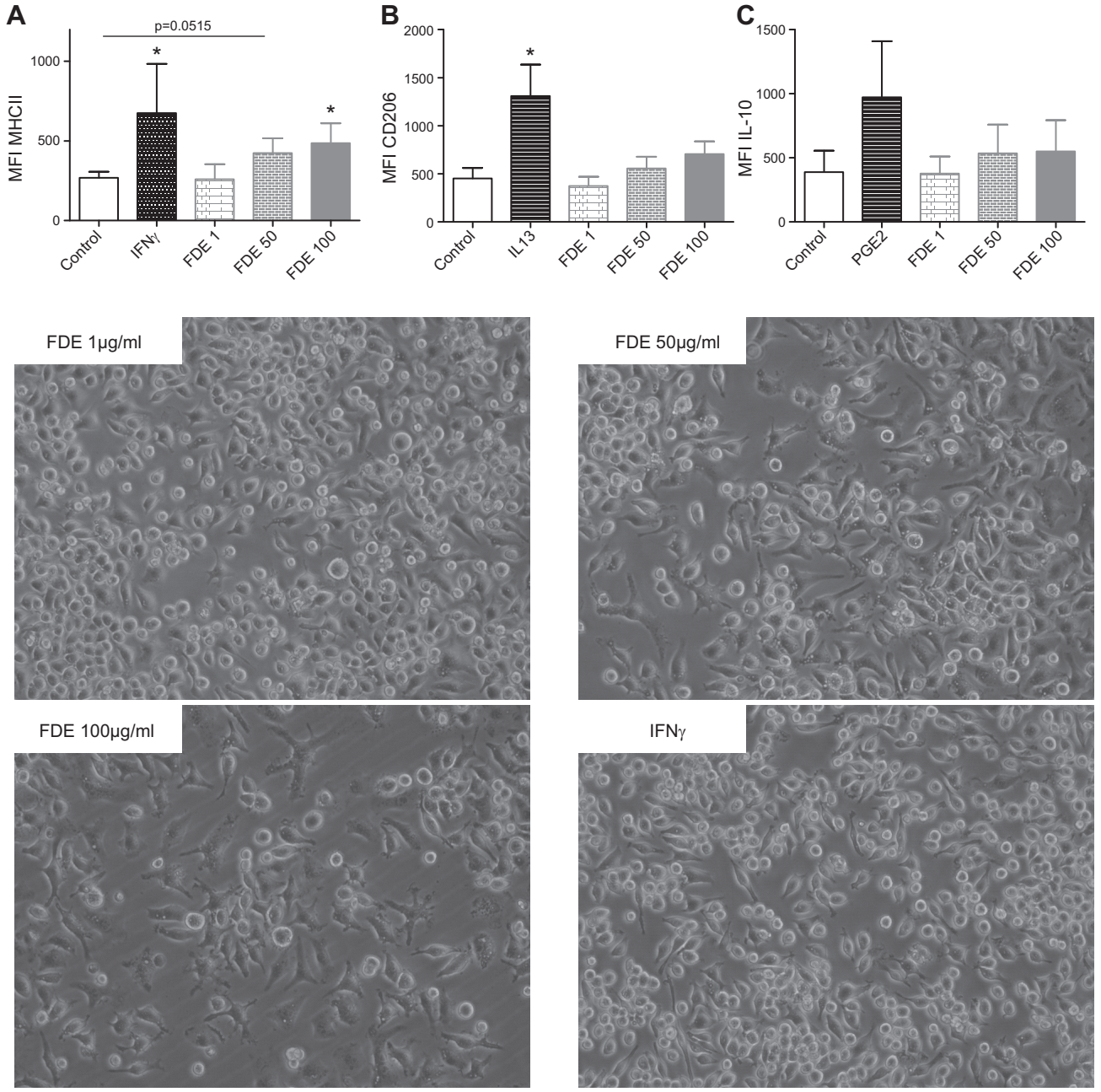

Fig. 5. FDE induces M1-dominant, but not M2-dominant or anti-inflammatory, macrophages. Bar graphs of expression of MHC II (*A*), CD206 (*B*), and IL-10 (*C*) of RAW cells stimulated with IFN-γ, IL-13, PGE2, or 3 different concentrations of FDE for 48 h. Each bar displays the mean and SD of 4 independent experiments. Representative pictures of RAW cells are shown from FDE and IFN-γ stimulations showing that FDE stimulation induces morphological changes similar to IFN-γ. *$P < 0.05$ compared with control.

place the IFN-γ produced by natural killer cells and T cells and induce M1-dominant polarization (14).

Conversely, M2-dominant macrophages are not directly polarized by HDM. Mouse alveolar macrophages recovered from BALF and stimulated in vitro with *Dermatophagoides farinae* showed an increase in TNF-α, IL-6, and nitric oxide production, all markers of M1-dominant polarization (2). This shows that M2-dominant polarization is dependent on IL-4 and/or IL-13 produced by other cell types. Considering the diversity of macrophage functions, M1-dominant macrophages would be needed directly after FDE exposure because of their enhanced phagocytosis and antigen presentation capabilities to accomplish microbial clearance, whereas M2-dominant macrophages are instructed at a later stage by the damaged tissue for repair purposes.

The role of M2-dominant macrophages in allergic asthma is still an ongoing debate, but it is thought that these cells could contribute to disease through secretion of extracellular matrix components and attraction of eosinophils (6). Correlations between asthma severity and numbers of M2-dominant macrophages or their products in lungs and serum of asthmatic patients (3, 12) and in mouse models (4) indicate that these

cells may actively contribute to disease. On the other hand, it has been shown in mice with abrogated IL-4 receptor-α signaling on macrophages that the M2-dominant phenotype is not necessary for allergic lung inflammation and may be a consequence of an elevated Th2 response (16). The finding that anti-inflammatory macrophages were found in lower numbers in HDM- and FDE-exposed mice compared with control mice indicates that this phenotype is prevalent in homeostasis and suggests, that during inflammation, polarization into other macrophage subsets occurs. One could speculate that, once microbial clearance is accomplished, a shift toward anti-inflammatory phenotype takes place to achieve resolution of inflammation.

In conclusion, in both nonallergic and allergic models of lung inflammation, high numbers of $CD11c^+/CD11b^+$ macrophages are induced in the lungs. The polarization status of these macrophages, however, is different depending on the environment, which determines the different types of inflammation in each model. In the nonallergic phenotype, the M1-dominant subset predominates, which may contribute via IRF5 to Th1-Th17 responses, whereas, in allergic conditions, the M2-dominant phenotype is more prevalent. This information may be important in the identification of new targets for therapeutic interventions in which skewing of macrophage polarization could be used as treatment for lung inflammation.

ACKNOWLEDGMENTS

The authors thank Annejet Spierenburg for the collection of farm dust samples, Jack Spithoven for the preparation of the farm dust extract, Pieter Klok for assistance with animal experiments, and Catharina Reker-Smith for help with the RAW cell experiments.

GRANTS

This work was supported by Grant no. 3.2.09.36 from The Netherlands Lung Foundation.

DISCLOSURES

No conflicts of interest, financial or otherwise, are declared by the authors.

AUTHOR CONTRIBUTIONS

Author contributions: P.R., C.D., W.T., I.M.W., B.N.M., and M.N.H. conception and design of research; P.R., C.D., T.R.B., and M.L. performed experiments; P.R., C.D., T.R.B., M.L., B.N.M., and M.N.H. analyzed data; P.R., C.D., T.R.B., M.L., W.T., I.M.W., B.N.M., and M.N.H. interpreted results of experiments; P.R. prepared figures; P.R. drafted manuscript; P.R., C.D., T.R.B., W.T., I.M.W., B.N.M., and M.N.H. edited and revised manuscript; P.R., C.D., T.R.B., M.L., W.T., I.M.W., B.N.M., and M.N.H. approved final version of manuscript.

REFERENCES

1. **Biswas SK, Mantovani A.** Macrophage plasticity and interaction with lymphocyte subsets: cancer as a paradigm. *Nat Immunol* 11: 889–896, 2010.
2. **Chen CL, Lee CT, Liu YC, Wang JY, Lei HY, Yu CK.** House dust mite Dermatophagoides farinae augments proinflammatory mediator productions and accessory function of alveolar macrophages: implications for allergic sensitization and inflammation. *J Immunol* 170: 528–536, 2003.
3. **Chupp GL, Lee CG, Jarjour N, Shim YM, Holm CT, He S, Dziura JD, Reed J, Coyle AJ, Kiener P, Cullen M, Grandsaigne M, Dombret MC, Aubier M, Pretolani M, Elias JA.** A chitinase-like protein in the lung and circulation of patients with severe asthma. *N Engl J Med* 357: 2016–2027, 2007.
4. **Draijer C, Robbe P, Boorsma CE, Hylkema MN, Melgert BN.** Characterization of macrophage phenotypes in three murine models of house-dust-mite-induced asthma. *Mediators Inflamm* 2013: 632049, 2013.
5. **Eduard W, Pearce N, Douwes J.** Chronic bronchitis, COPD, and lung function in farmers: the role of biological agents. *Chest* 136: 716–725, 2009.
6. **Ford AQ, Dasgupta P, Mikhailenko I, Smith EM, Noben-Trauth N, Keegan AD.** Adoptive transfer of IL-4Ralpha+ macrophages is sufficient to enhance eosinophilic inflammation in a mouse model of allergic lung inflammation. *BMC Immunol* 13: 6-2172-13-6, 2012.
7. **Hong JY, Chung Y, Steenrod J, Chen Q, Lei J, Comstock AT, Goldsmith AM, Bentley JK, Sajjan US, Hershenson MB.** Macrophage activation state determines the response to rhinovirus infection in a mouse model of allergic asthma. *Respir Res* 15: 63-9921-15-63, 2014.
8. **Johnston LK, Rims CR, Gill SE, McGuire JK, Manicone AM.** Pulmonary macrophage subpopulations in the induction and resolution of acute lung injury. *Am J Respir Cell Mol Biol* 47: 417–426, 2012.
9. **Krausgruber T, Blazek K, Smallie T, Alzabin S, Lockstone H, Sahgal N, Hussell T, Feldmann M, Udalova IA.** IRF5 promotes inflammatory macrophage polarization and TH1-TH17 responses. *Nat Immunol* 12: 231–238, 2011.
10. **Kurowska-Stolarska M, Stolarski B, Kewin P, Murphy G, Corrigan CJ, Ying S, Pitman N, Mirchandani A, Rana B, van Rooijen N, Shepherd M, McSharry C, McInnes IB, Xu D, Liew FY.** IL-33 amplifies the polarization of alternatively activated macrophages that contribute to airway inflammation. *J Immunol* 183: 6469–6477, 2009.
11. **Melgert BN, Oriss TB, Qi Z, Dixon-McCarthy B, Geerlings M, Hylkema MN, Ray A.** Macrophages: regulators of sex differences in asthma? *Am J Respir Cell Mol Biol* 42: 595–603, 2010.
12. **Melgert BN, ten Hacken NH, Rutgers B, Timens W, Postma DS, Hylkema MN.** More alternative activation of macrophages in lungs of asthmatic patients. *J Allergy Clin Immunol* 127: 831–833, 2011.
13. **Moreira AP, Cavassani KA, Hullinger R, Rosada RS, Fong DJ, Murray L, Hesson DP, Hogaboam CM.** Serum amyloid P attenuates M2 macrophage activation and protects against fungal spore-induced allergic airway disease. *J Allergy Clin Immunol* 126: 712–721; e7, 2010.
14. **Mosser DM, Edwards JP.** Exploring the full spectrum of macrophage activation. *Nat Rev Immunol* 8: 958–969, 2008.
15. **Nagarkar DR, Bowman ER, Schneider D, Wang Q, Shim J, Zhao Y, Linn MJ, McHenry CL, Gosangi B, Bentley JK, Tsai WC, Sajjan US, Lukacs NW, Hershenson MB.** Rhinovirus infection of allergen-sensitized and -challenged mice induces eotaxin release from functionally polarized macrophages. *J Immunol* 185: 2525–2535, 2010.
16. **Nieuwenhuizen NE, Kirstein F, Jayakumar J, Emedi B, Hurdayal R, Horsnell WG, Lopata AL, Brombacher F.** Allergic airway disease is unaffected by the absence of IL-4Ralpha-dependent alternatively activated macrophages. *J Allergy Clin Immunol* 130: 743–750; e8, 2012.
17. **Poole JA, Alexis NE, Parks C, MacInnes AK, Gentry-Nielsen MJ, Fey PD, Larsson L, Allen-Gipson D, Von Essen SG, Romberger DJ.** Repetitive organic dust exposure in vitro impairs macrophage differentiation and function. *J Allergy Clin Immunol* 122: 375–382; e1–e4, 2008.
18. **Poole JA, Gleason AM, Bauer C, West WW, Alexis N, Reynolds SJ, Romberger DJ, Kielian T.** alphabeta T cells and a mixed Th1/Th17 response are important in organic dust-induced airway disease. *Ann Allergy Asthma Immunol* 109: 266–273: e2, 2012.
19. **Poole JA, Gleason AM, Bauer C, West WW, Alexis N, van Rooijen N, Reynolds SJ, Romberger DJ, Kielian TL.** CD11c(+)/CD11b(+) cells are critical for organic dust-elicited murine lung inflammation. *Am J Respir Cell Mol Biol* 47: 652–659, 2012.
20. **Poole JA, Kielian T, Wyatt TA, Gleason AM, Stone J, Palm K, West WW, Romberger DJ.** Organic dust augments nucleotide-binding oligomerization domain expression via an NF-κB pathway to negatively regulate inflammatory responses. *Am J Physiol Lung Cell Mol Physiol* 301: L296–L306, 2011.
21. **Poole JA, Wyatt TA, Kielian T, Oldenburg P, Gleason AM, Bauer A, Golden G, West WW, Sisson JH, Romberger DJ.** Toll-like receptor 2 regulates organic dust-induced airway inflammation. *Am J Respir Cell Mol Biol* 45: 711–719, 2011.
22. **Poole JA, Wyatt TA, Oldenburg PJ, Elliott MK, West WW, Sisson JH, Von Essen SG, Romberger DJ.** Intranasal organic dust exposure-induced airway adaptation response marked by persistent lung inflammation and pathology in mice. *Am J Physiol Lung Cell Mol Physiol* 296: L1085–L1095, 2009.
23. **Raes G, De Baetselier P, Noel W, Beschin A, Brombacher F, Hassanzadeh Gh G.** Differential expression of FIZZ1 and Ym1 in alternatively versus classically activated macrophages. *J Leukoc Biol* 71: 597–602, 2002.

24. **Ray A, Khare A, Krishnamoorthy N, Qi Z, Ray P.** Regulatory T cells in many flavors control asthma. *Mucosal Immunol* 3: 216–229, 2010.
25. **Robbe P, Spierenburg E, Draijer C, Brandsma C, Telenga E, van Oosterhout A, van den Berge M, Luinge M, Melgert B, Heederik D, Timens W, Wouters I, Hylkema M.** Shifted T-cell polarisation after agricultural dust exposure in mice and men. *Thorax* 69: 630–637, 2014.
26. **Stein M, Keshav S, Harris N, Gordon S.** Interleukin 4 potently enhances murine macrophage mannose receptor activity: a marker of alternative immunologic macrophage activation. *J Exp Med* 176: 287–292, 1992.
27. **Weiss M, Blazek K, Byrne AJ, Perocheau DP, Udalova IA.** IRF5 is a specific marker of inflammatory macrophages in vivo. *Mediators Inflamm* 2013: 245804, 2013.
28. **Xue J, Schmidt SV, Sander J, Draffehn A, Krebs W, Quester I, De Nardo D, Gohel TD, Emde M, Schmidleithner L, Ganesan H, Nino-Castro A, Mallmann MR, Labzin L, Theis H, Kraut M, Beyer M, Latz E, Freeman TC, Ulas T, Schultze JL.** Transcriptome-based network analysis reveals a spectrum model of human macrophage activation. *Immunity* 40: 274–288, 2014.
29. **Yamamoto M, Sato S, Hemmi H, Hoshino K, Kaisho T, Sanjo H, Takeuchi O, Sugiyama M, Okabe M, Takeda K, Akira S.** Role of adaptor TRIF in the MyD88-independent Toll-like receptor signaling pathway. *Science* 301: 640–643, 2003.
30. **Yu S, Kim HY, Chang YJ, DeKruyff RH, Umetsu DT.** Innate lymphoid cells and asthma. *J Allergy Clin Immunol* 133: 943–50; quiz 51, 2014.